Journal of Biomolecular NMR, 1 (1991) 439–446
ESCOM

J-Bio NMR 038

Measurement of ^{15}N-^{13}C J couplings in staphylococcal nuclease

Frank Delaglio[a], Dennis A. Torchia[b] and Ad Bax[a]

[a]*Laboratory of Chemical Physics, National Institute of Diabetes and Digestive and Kidney Diseases, National Institutes of Health, Bethesda, MD 20892, U.S.A.*
[b]*Bone Research Branch, National Institute of Dental Research, National Institutes of Health, Bethesda, MD 20892, U.S.A.*

Dedicated to the memory of Professor V.F. Bystrov

Received 15 July 1991
Accepted 12 August 1991

Keywords: 2D NMR; J couplings; Protein structure; Isotopic labeling; Triple resonance

SUMMARY

^{15}N-Cα and ^{15}N-C′ J couplings were measured for the backbone of staphylococcal nuclease, uniformly enriched with ^{15}N and ^{13}C. It is found that the $^{1}J_{C'N}$ coupling is similar for β-sheet, J = 14.8 ± 0.5 and for α-helix, J = 14.8 ± 0.4 but tends to be larger for the unstructured N- and C-terminal ends of the protein (J = 15.6 ± 0.5). On average, $^{1}J_{NC\alpha}$ are smaller for α-helical residues (J = 9.6 ± 0.3 Hz) compared to β-sheet (J = 10.9 ± 0.8 Hz) and a substantial difference is observed for $^{2}J_{NC\alpha}$ in α-helices (J = 6.4 ± 0.4 Hz) and β-sheets (J = 8.3 ± 0.8 Hz).

INTRODUCTION

The use of spin-spin coupling constants for obtaining structural information of biologically active peptides has been explored extensively by Bystrov (1976). Homonuclear ^{1}H-^{1}H couplings have been especially useful for studying protein conformation and for making stereospecific assignments of Cβ methylene protons in proteins. Measurement of multiple bond ^{1}H-^{13}C and ^{1}H-^{15}N J couplings in proteins has become feasible with the use of isotopic enrichment (Montelione et al., 1989; Wider et al., 1989; Edison et al., 1991) providing access to an important source of structural information (Bystrov, 1976).

Recently developed triple resonance NMR techniques for obtaining backbone and side-chain assignments in isotopically enriched proteins rely on magnetization transfer via $^{1}J_{NC}$ and $^{2}J_{NC}$ couplings (Ikura et al., 1990; Kay et al., 1990). Very few data are available in the literature regarding the size of these couplings. Bystrov (1976) reports values for peptides of $^{1}J_{NC\alpha} \sim 11$ Hz and

$^2J_{NC\alpha} \sim 7$ Hz. Kopple et al. (1978) reported values of 11.0 and 7.2 Hz for a dipeptide analog. Intensities in the triple resonance experiments we conducted were found to vary significantly and therefore we found it of interest to investigate the degree of variation found for these one- and two-bond nitrogen-carbon J couplings.

Two of the triple resonance experiments which rely on magnetization transfer via $^1J_{NC}$ and $^2J_{NC}$ are known as HNCO and HNCA. The HNCO experiment correlates along the orthogonal axes of a 3D spectrum the chemical shifts of the amide proton, ^{15}N and carbonyl for each peptide bond in the protein (with the exception of peptide bonds preceding proline or that have rapidly exchanging amide protons). The HNCA experiment correlates in a similar manner the amide proton and ^{15}N shifts with both the intraresidue Cα resonance (via $^1J_{NC\alpha}$) and the Cα of the preceding residue (via $^2J_{NC\alpha}$). Particularly the interresidue H-N-Cα correlations were found to vary widely in intensity. Although the intraresidue H-N-Cα correlation for a given amide usually is more intense than the interresidue connectivity, several possible exceptions have also been noted (Powers et al., 1991).

EXPERIMENTAL APPROACH

Here we report a simple technique for measuring the J_{NC} couplings in an accurate manner and demonstrate the technique for a 1.5 mM sample of the protein staphylococcal nuclease (149 resi-

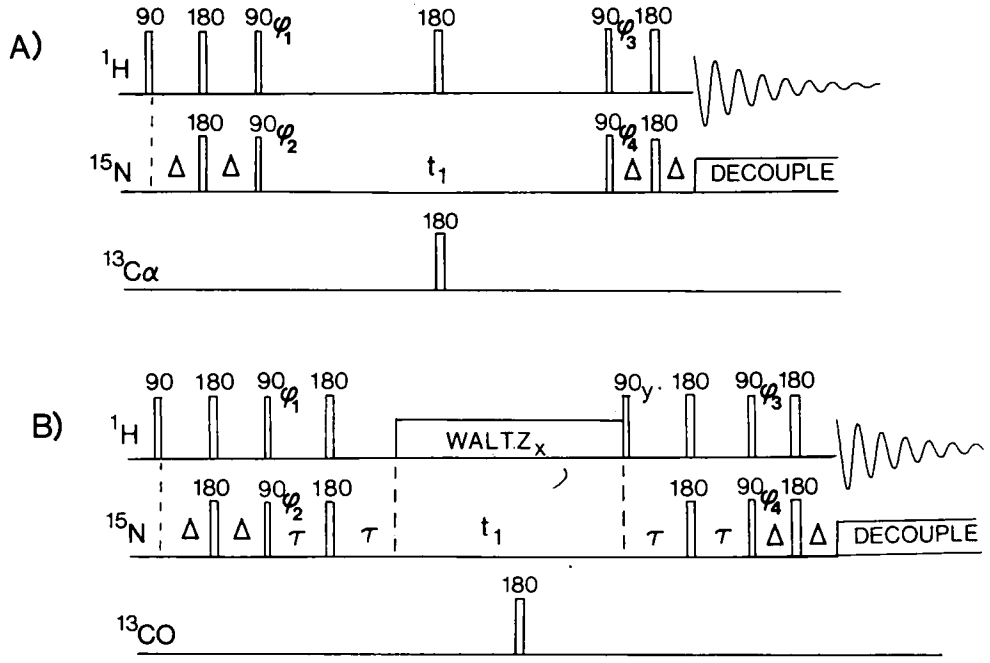

Fig. 1. Pulse schemes used for measuring the (A) $J_{NC'}$ coupling and (B) the $J_{NC\alpha}$ couplings. The WALTZ decoupling during the t_1 period, followed immediately by the 90_y ^1H purge pulse suppresses signals from NH_2 groups and can, of course, also be used for scheme (A) where the $^{13}C\alpha$ carbons are decoupled during the t_1 period. The phase cycling used is as follows: $\varphi_1 = y, -y$; $\varphi_2 = 4(x),4(-x)$; $\varphi_3 = 2(x),2(-x)$; $\varphi_4 = 8(x),8(-x)$; Acq. $= x,2(-x),x,-x,2(x),-x,-x,2(x),-x,x,2(-x),x$. Quadrature in the t_1 dimension is accomplished using time proportional phase incrementation (TPPI) of φ_2.

dues) complexed with Ca^{2+} and pdTp, and uniformly enriched with both ^{15}N and ^{13}C. Complete resonance assignments of this complex were obtained previously (Torchia et al., 1989; Wang et al., 1990a,b; Baldisseri et al., 1991). A high-resolution X-ray crystal structure is also available (Loll and Lattman, 1989). Using the crystallographic data, we here present evidence for possible correlations between the J_{NC} couplings and protein structure.

The $^1J_{NC}$ splittings can be observed in a regular Overbodenhausen (Bodenhausen and Ruben, 1980; Bax et al., 1990) (HSQC) ^1H-^{15}N correlation spectrum of a protein that has been uniformly enriched with both ^{13}C and ^{15}N. However, because the backbone ^{15}N nucleus in a protein has significant J couplings with three different ^{13}C nuclei, the multiplet structure is frequently unresolved. Simplification can be obtained if either the $^{13}C\alpha$ resonances are decoupled during the evo-

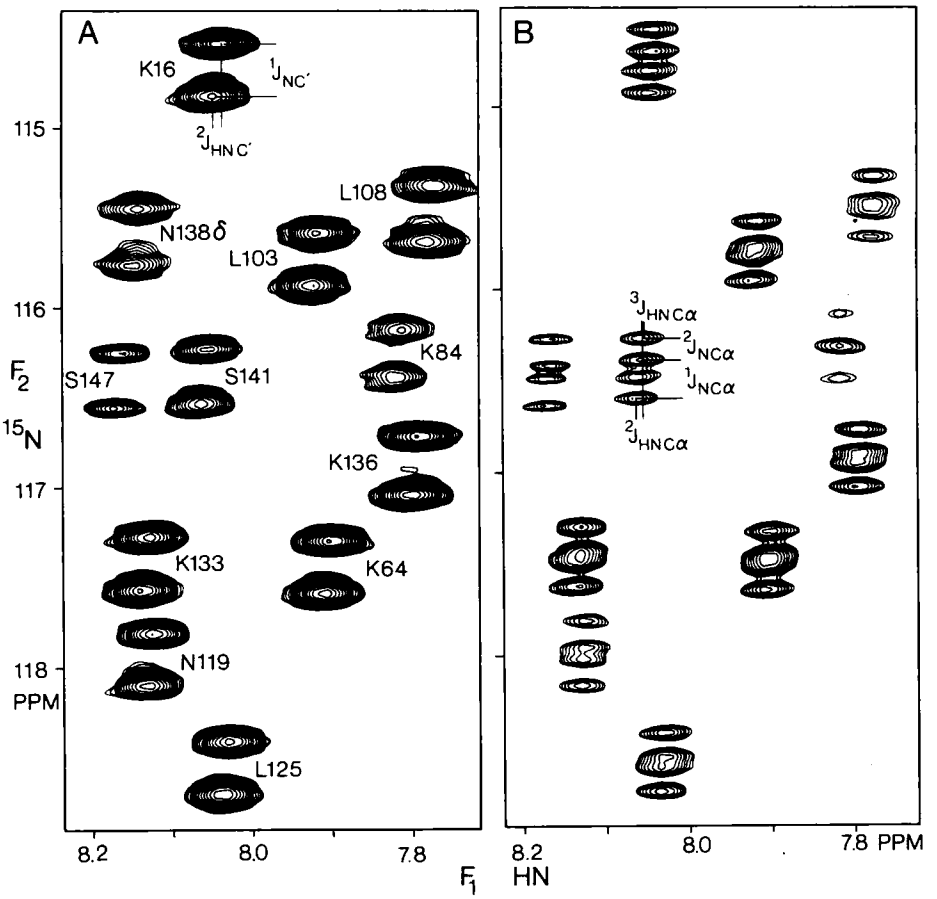

Fig. 2. Regions from the ^1H-^{15}N shift correlation spectra recorded for a 1.5 mM solution of staphylococcal nuclease complexed with pdTp and Ca^{2+}, using (A) the sequence of Fig. 1A and (B) the pulse scheme of Fig. 1B. Acquisition times were 200 ms (t_1) and 64 ms (t_2), and the total measuring time was 18 h per spectrum. For the WALTZ decoupling during t_1 a 2.5 kHz ^1H RF field was used. Other ^1H pulses were applied using a 16 kHz RF field. Presaturation of the H_2O resonance using a 25 Hz RF field was employed for both experiments during the delay time between scans. Data were processed with Lorentzian to Gaussian transformation filters and stronger filtering was used for (B) than for (A). Data were zero filled in both dimensions to yield a digital resolution of 0.4 Hz (F_1) and 7.8 Hz (F_2).

lution period of the experiment (Fig. 1A), resulting in a doublet with the $^1J_{NC'}$ splitting, or if the carbonyl is decoupled (Fig. 1B) which then results in a doublet of doublets showing the $^1J_{NC\alpha}$ and $^2J_{NC\alpha}$ splittings. As discussed previously (Bax et al., 1990) the highest resolution in the ^{15}N dimension is obtained if the protons are decoupled by a composite pulse decoupling scheme, as shown in Fig. 1B, instead of by a single 180° ^1H pulse at the midpoint of t_1 (Fig. 1A). The 90° pulse at the end of the WALTZ composite pulse decoupling must be 90° out of phase relative to the (lower power) decoupling field, in order to eliminate spurious t_1-noise like artifacts originating from the NH_2 moieties.

Figure 2 shows identical regions of the ^1H-^{15}N shift correlation spectrum obtained (A) with the pulse scheme of Fig. 1A, showing the ^{15}N-C′ J couplings, and (B) obtained with the scheme of Fig. 1B, showing the one- and two-bond ^{15}N-Cα splittings. In principle, one might expect that other two- and three-bond J couplings between ^{15}N and Cβ, Cγ and C′ nuclei, or between ^{15}N nuclei of adjacent residues also could give rise to observable splittings. In practice these J couplings are apparently quite small since no evidence for significant line broadening over the values expected based on T_2 measurements (Kay et al., 1989) was observed.

The $^1J_{NC'}$ J splittings can be measured simply by peak picking of the spectrum of Fig. 2A. Many of the $J_{NC\alpha}$ cannot be measured in a similar fashion because the center two components of the multiplet frequently are unresolved (Fig. 2B). To obtain accurate J values for the partially resolved multiplets, a constrained surface fitting program was developed (Delaglio, to be published) which assumes that all four multiplet components have identical intensity and line width in both the F_1 and F_2 dimension, and that the heteronuclear $^3J_{H\alpha N}$ and $^2J_{H\alpha N}$ couplings are both smaller than 6 Hz. Different parametrization of the same program makes it suitable for accurate measurement of the $^1J_{NC'}$ coupling. Couplings measured for the resolved multiplets using the constrained surface fitting program never deviated by more than 0.25 Hz (for $J_{NC\alpha}$) and 0.12 Hz (for $J_{NC'}$) from the peak picking results. Therefore, all couplings reported here have been measured with the constrained fitting procedure.

The spectra shown in Fig. 2 were recorded twice and only values that reproduced better than 0.3 Hz are reported here. Residues for which the surface fitting did not show good convergence (frequently because of partial overlap with other amides), or for which the amide proton was strongly attenuated by the H_2O presaturation are also not considered. It is assumed below that the smaller of the two $J_{NC\alpha}$ couplings corresponds to $^2J_{NC\alpha}$. Exceptions to this rule may occur in rare instances but in these cases the magnitudes of the two couplings are invariably quite close.

RESULTS AND DISCUSSION

The J values obtained for staphylococcal nuclease are presented in Table 1, along with the relevant φ, ψ and ω angles obtained from the 1.65 Å crystal structure refined to an R factor of 17% (Loll and Lattman, 1989). Averaged over all residues we find $^1J_{NC'} = 15.0 \pm 0.7$ Hz, $^1J_{NC\alpha} = 10.5 \pm 0.9$ Hz and $^2J_{NC\alpha} = 7.5 \pm 1.1$ Hz. A substantial number of residues for which J values were measured are part of canonical α-helices and β-sheets. In addition, previous NMR studies have shown that residues prior to His[8] and succeeding Ser[141] adopt an unstructured random coil type conformation. The average J values and their standard deviations are as follows:

α-helix: $^1J_{NC'} = 14.8 \pm 0.4$ Hz (N = 24); $^1J_{NC\alpha} = 9.6 \pm 0.3$ Hz (N = 14);
$^2J_{NC\alpha} = 6.4 \pm 0.4$ Hz (N = 14).

TABLE 1
J_{CN} COUPLINGS AND BACKBONE TORSION ANGLES IN STAPHYLOCOCCAL NUCLEASE

	ψ^a_{i-1}	ω^a	φ^a	$^1J_{NC'}$	$^2J_{NC\alpha}$	$^1J_{NC\alpha}$		ψ^a_{i-1}	ω^a	φ^a	$^1J_{NC'}$	$^2J_{NC\alpha}$	$^1J_{NC\alpha}$
Lys[6]				15.4	7.2	11.2	Lys[84]	178	−175.9	−61	13.5	7.9	9.8
Leu[7]			−180	15.3	8.0	11.2	Tyr[85]	−11	179.4	−96	15.8	5.7	10.1
His[8]			−134	14.4			Gly[86]	−0	−177.8	82	16.4	6.2	10.7
Lys[9]	138	178.5	−86	15.3	8.7	10.8	Arg[87]	16	180.0	−88	16.4	6.4	11.1
Glu[10]	146	176.0	−133	15.0	8.8	11.4	Leu[89]	145	178.0	−110	15.1	8.8	10.5
Thr[13]	160	179.4	−120	15.5	8.5	12.6	Ala[90]	108	−178.2	−149	14.2	8.6	12.3
Leu[14]	131	−179.2	−62	14.6	8.0	11.1	Tyr[91]	171	167.8	−95	14.9	8.7	11.1
Lys[16]	−58	−178.9	−166	14.7	6.1	11.5	Ile[92]	130	−179.6	−111	14.5		
Ala[17]	135	178.6	−81	14.6	8.1	10.4	Tyr[93]	136	−179.4	−118	15.3	8.8	11.1
Ile[18]	132	−179.2	−98	14.5	8.2	9.3	Ala[94]	139	178.5	−119	14.2	8.8	9.6
Asp[19]	−48	178.2	−156	15.7	6.2	12.8	Asp[95]	110	−178.9	52	14.2	8.4	9.2
Asp[21]	−34	−174.5	−122		6.3	10.8	Gly[96]	42	175.9	76	15.3		
Thr[22]	12	−178.5	−137	16.0			Lys[97]	9	178.5	−106	16.1		
Val[23]	130	179.5	−142	14.8	8.1	11.4	Met[98]	128	−179.0	−70	13.9	8.8	9.9
Lys[24]	148	177.7	−97	15.1	8.2	10.3	Val[99]	117	178.6	−62	14.6		
Leu[25]	129	−178.5	−131	15.0	8.4	11.4	Asn[100]	−40	−176.5	−54	13.4	6.7	9.1
Met[26]	157	173.7	−97	14.3	8.6	9.8	Glu[101]	−44	−176.1	−74	14.7	7.6	9.2
Tyr[27]	120	−177.2	−133	14.0	8.1	9.9	Ala[102]	−39	179.4	−55	15.5		
Lys[28]	118	179.9	58	14.4	8.0	9.1	Leu[103]	−44	178.6	−60	14.7	6.4	9.8
Gly[29]	39	−179.2	72	15.3			Val[104]	−49	179.6	−62	14.6		
Met[32]	133	178.8	−150	15.2	9.0	11.0	Arg[105]	−48	−178.7	−56	14.8		
Thr[33]	153	173.9	−101	15.0	8.5	10.8	Gln[106]	−32	−179.7	−87	14.8	6.4	10.1
Phe[34]	131	179.5	−107	15.1	8.2	11.2	Gly[107]	−1	−179.0	75	15.3	6.2	10.4
Arg[35]	142	174.3	−116	14.1	8.5	10.6	Leu[108]	25	179.3	−102	15.8	6.7	10.2
Leu[37]	124	175.1	−65	14.3			Ala[109]	5	−179.8	−163		6.6	12.2
Leu[38]	151	172.7	58	14.5	8.9	8.9	Val[111]	155	174.5	−75	14.8	8.2	10.1
Thr[41]	113	175.7	−96	14.8	8.5	11.2	Ala[112]	125	−178.4	−148	15.7	7.5	12.2
Ala[58]	−45	178.0	−61	15.2			Tyr[113]	172	173.0	53	15.1	9.0	10.2
Ser[59]	−43	−177.3	−63	14.4	6.8	10.2	Tyr[115]	109	178.8	−122	14.4	7.8	10.0
Ala[60]	−43	−177.3	−65	15.3			Lys[116]	108	176.7	−64	13.9	8.1	11.1
Phe[61]	−40	−178.2	−60	15.3	6.2	9.3	Asn[118]	16	−177.6	−84	15.1	6.0	9.0
Lys[64]	−54	−177.8	−55	14.6	6.5	9.8	Asn[119]	65	−177.3	−144	14.5	7.1	10.7
Val[66]	−49	−177.1	−79	14.7	6.3	9.8	Thr[120]	31	−178.1	−53	15.1		
Asn[68]	−31	−178.7	−86	14.8	6.3	10.3	His[121]	−43	−174.5	−102		5.8	10.5
Ala[69]	−5	−176.7	−73	16.8	6.3	11.7	Glu[122]	22	−179.1	−56	14.9	6.3	9.1
Lys[70]	142	172.2	−72	14.7	8.4	9.5	Gln[123]	−46	−178.3	−64	14.3	6.3	9.6
Lys[71]	−49	−175.9	−126	15.4	6.2	10.5	His[124]	−44	176.2	−56	14.5		
Ile[72]	137	174.5	−117	15.1	8.3	10.6	Leu[125]	−53	176.8	−61	14.7	6.3	9.7
Glu[73]	140	176.3	−135	14.1	8.3	11.5	Arg[126]	−38	−179.2	−65	14.5		
Val[74]	147	179.5	−116	15.1	8.6	10.9	Ser[128]	−39	180.0	−63	15.0	6.1	9.7
Glu[75]	140	177.6	−129		8.7	9.0	Glu[129]	−38	−179.4	−64	14.9		
Phe[76]	111	179.8	−78	14.7	7.8	11.2	Ala[130]	−40	−179.8	−62	14.5	6.3	9.9
Asp[77]	156	177.7	−91	15.1	9.0	12.0	Gln[131]	−39	177.7	−65	15.3	6.1	9.5
Lys[78]	−166	−176.1	−92	13.1	7.9	9.6	Ala[132]	−46	176.6	−60	14.7		
Gly[79]	−9	177.7	−102	16.9	6.2	12.2	Lys[133]	−39	−179.9	−66	14.9	6.6	10.0
Gln[80]	−145	178.3	−56	15.2	9.5	11.4	Lys[134]	−49	179.4	−68	14.5	5.9	9.6
Thr[82]	−3	178.9	−137	16.0	6.4	12.3	Lys[136]	3	178.3	51	16.5	6.1	9.6
Asp[83]	151	176.4	−96		8.3	12.6	Asn[138]	135	176.3	40	13.3	9.6	9.0[b]

TABLE I (continued)

	ψ^{a}_{i-1}	ω^{a}	φ^{a}	$^{1}J_{NC'}$	$^{2}J_{NC\alpha}$	$^{1}J_{NC\alpha}$		ψ^{a}_{i-1}	ω^{a}	φ^{a}	$^{1}J_{NC'}$	$^{2}J_{NC\alpha}$	$^{1}J_{NC\alpha}$
Ser[141]	2	−175.5	−79	15.3	5.9	10.7	Asp[146]				15.3	7.4	10.6
Glu[142]				15.8			Ser[147]				15.4	7.5	11.0
Asp[143]				15.0	7.7	10.5	Gly[148]				16.1	6.8	10.2
Asn[144]				15.1	7.8	10.5	Gln[149]				16.7	7.6	10.3
Ala[145]				15.7	7.4	10.1							

[a] Backbone angles have been derived from the X-ray crystal structure coordinates (Loll and Lattman, 1989) which are present in the Brookhaven Protein Data Bank.

[b] Analysis of the relative intensities of intra- and interresidue connectivities in the HNCA spectrum of staphylococcal nuclease (H.R.C. Cole, unpublished) indicates that for Asn[138] $^{2}J_{NC\alpha} > {}^{1}J_{NC\alpha}$. For all other residues $^{2}J_{NC\alpha} \leq {}^{1}J_{NC\alpha}$.

β-sheet: $^{1}J_{NC'} = 14.8 \pm 0.5$ Hz (N = 20); $^{1}J_{NC\alpha} = 10.9 \pm 0.8$ Hz (N = 20);
$^{2}J_{NC\alpha} = 8.3 \pm 0.8$ Hz (N = 20).

r. coil: $^{1}J_{NC'} = 15.6 \pm 0.5$ Hz (N = 10); $^{1}J_{NC\alpha} = 10.6 \pm 0.4$ Hz (N = 9);
$^{2}J_{NC\alpha} = 7.5 \pm 0.4$ Hz (N = 9).

The fact that even for residues in a random coil type conformation there is a significant spread in the measured J values suggests that the size of the J couplings varies with the types of amino acids involved in the peptide bond. However, certain significant trends, correlating the J values with structural parameters are also apparent.

The $^{1}J_{NC'}$ coupling is of a similar magnitude in both α-helix and β-sheet, and significantly smaller than for random coil type conformations. Although no correlation with secondary structure is found, inspection of Table I shows that out of all peptide bonds for which $^{1}J_{NC'} \geq 16$ Hz (N = 10), seven are preceded by a ψ angle in the range $-9° < \psi < 12°$. Three residues with a $J_{NC'}$ coupling larger than 16 Hz that are not preceded by a ψ angle in this range are Arg[87] ($\psi_{i-1} = 16°$) and the two C-terminal residues, Gly[148] and Glu[149]. The peptide bonds preceding Gly[107] and Ser[141] (the last residue for which intensity is observed in the X-ray study) are preceded by ψ angles in this range but have $^{1}J_{NC'} < 16$ Hz.

A possible correlation between the magnitude of the $^{1}J_{NC'}$ coupling and the non-planarity of the peptide bond, i.e. the deviation from 180°, has been suggested (Kainosho et al., 1987). The present data provide no supporting evidence for this hypothesis although it should be kept in mind that the uncertainty in the crystallographically determined ω angles may mask any such correlation.

Inspection of the $^{1}J_{NC\alpha}$ values shows that this coupling is substantially larger in β-sheet compared to α-helix. An even more significant difference is observed for $^{2}J_{NC\alpha}$. Figure 3 shows a graphic correlation between the $^{2}J_{NC\alpha}$ values and ψ. Clearly, ψ values in the range of −60° to +30° give rise to significantly smaller two-bond couplings than ψ angles in the 100°–180° range. Residues in β-sheets are thus expected to have also considerably larger $^{2}J_{NC\alpha}$ values compared to residues in α-helices. Lys[16] is an apparent exception to this rule, with a $^{2}J_{NC\alpha}$ value of 7 Hz. However, Loll and Lattman have noted that Ile[15] and Lys[16] form a β-bulge and the β-sheet is strongly distorted at this position, with a ψ angle of −58° preceding the peptide bond.

Our results indicate that one- and two-bond J_{NC} couplings are correlated with protein backbone conformation. A much larger database, however, must be analyzed before these J couplings

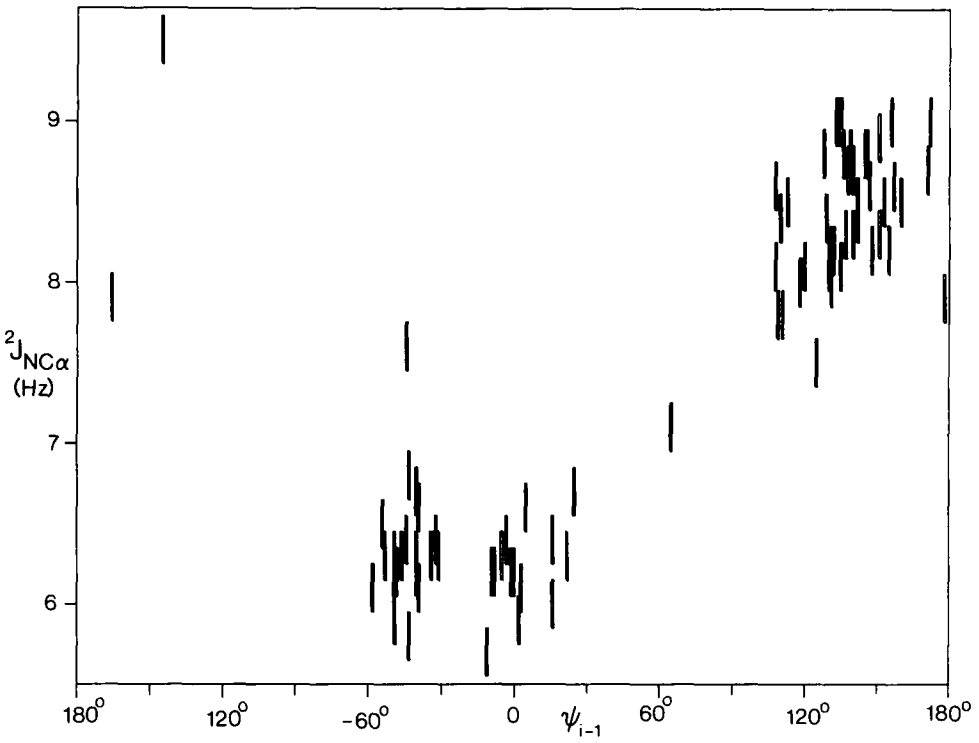

Fig. 3. Correlation between the measured $^2J_{NC\alpha}$ coupling and the backbone angle ψ in the protein staphylococcal nuclease. J values were obtained by constrained surface fitting of the spectrum for which a section is shown in Fig. 2B.

can be used as structural parameters in the same way as $^3J_{HH}$ couplings are now routinely used. As we have shown, measurement of the J_{NC} couplings is very straightforward for isotopically enriched proteins and it may be anticipated that the use of both homonuclear and heteronuclear J couplings will find increasing importance in protein structural studies. We are grateful to Vladimir Bystrov for his seminal work which has stimulated the many subsequent developments in this field.

ACKNOWLEDGEMENTS

We thank Mike Barfield for stimulating discussions and suggestions, and for sending us previously unpublished data recorded for model compounds. This work was supported by the AIDS-directed anti-viral program of the Office of the Director of the National Institutes of Health.

REFERENCES

Baldisseri, D.M., Torchia, D.A., Poole, L.B. and Gerlt, J.A. (1991) *Biochemistry*, **30**, 3628–3633.
Bax, A., Ikura, M., Kay, L.E., Torchia, D.A. and Tschudin, R. (1990) *J. Magn. Reson.*, **86**, 304–318.
Bodenhausen, G. and Ruben, D.J. (1980) *Chem. Phys. Lett.*, **69**, 185–188.
Bystrov, V.F. (1976) *Progr. NMR Spectrosc.*, **10**, 44–81.
Edison, A.S., Westler, W.M. and Markley, J.L. (1991) *J. Magn. Reson.*, **92**, 434–438.

Ikura, M., Kay, L.E. and Bax, A. (1990) *Biochemistry*, **29**, 4659–4667.
Kainosho, M., Nagao, H. and Tsuji, T. (1987) *Biochemistry*, **26**, 1068–1075.
Kay, L.E., Torchia, D.A. and Bax, A. (1989) *Biochemistry*, **28**, 8972–8979.
Kay, L.E., Ikura, M., Tschudin, R. and Bax, A. (1990) *J. Magn. Reson.*, **89**, 496–514.
Kopple, K.D., Ashan, A. and Barfield, M. (1978) *Tetrahedron Lett.*, **38**, 3519–3522.
Loll, P.J..and Lattman, E.E. (1989) *Proteins: Struct., Funct. Genet.*, **5**, 183–201.
Montelione, G.T., Winkler, M.E., Rauenbuhler, P. and Wagner, G. (1989) *J. Magn. Reson.*, **82**, 198–204.
Powers, R., Clore, G.M., Bax, A., Garrett, D.S., Stahl, P.T. and Gronenborn, A.M. (1991) *J. Mol. Biol.*, in press
Torchia, D.A., Sparks, S.W. and Bax, A. (1989) *Biochemistry*, **28**, 5509–5524.
Wang, J., LeMaster, D.M. and Markley, J.L. (1990a) *Biochemistry*, **29**, 88–101.
Wang, J., Hinck, A.P., Loh, S.N. and Markley, J.L. (1990b) *Biochemistry*, **29**, 102–113.
Wider, G., Neri, D., Otting, G. and Wüthrich, K. (1989) *J. Magn. Reson.*, **85**, 426–431.